

Measurements of discrete electronic states in a gold nanoparticle using tunnel junctions formed from self-assembled monolayers

Jason R. Petta,^{a)} D. G. Salinas, and D. C. Ralph

Laboratory of Atomic and Solid State Physics, Cornell University, Ithaca, New York 14853

(Received 17 May 2000; accepted for publication 27 October 2000)

We present results from nanometer-scale tunnel junctions fabricated using organic self-assembled monolayers (SAMs) as tunnel barriers. Single junctions have resistances consistent with tunneling through a single layer of molecules. In several devices, a gold nanoparticle nucleated within the SAM barrier. Such samples allow a sensitive test of mechanical stability—some are sufficiently stable to permit the observation of electron tunneling through individual electron-in-a-box states at low voltages and mK temperatures. We also observe anomalous transport characteristics at larger voltages, which may be due to the motion of the gold nanoparticle within the monolayer. © 2000 American Institute of Physics. [S0003-6951(00)04751-3]

The process of self-assembly, when used in conjunction with lithographic techniques, has made it possible to study the properties of single molecules and chemically synthesized nanoparticles. By fabricating leads with nanometer separation, several groups have been able to perform tunneling spectroscopy measurements on single semiconducting or metallic nanocrystals passivated with an organic capping layer.^{1–3} Zhou *et al.* have studied devices in which self-assembled monolayers (SAMs) are used to create molecular diodes.⁴ More recently, Collier *et al.* have fabricated logic gates using a Langmuir–Blodgett film.⁵ The self-assembly process provides great flexibility since one can tailor the electronic properties of a device by choosing the desired molecule.

In this letter, we present measurements performed on devices fabricated using self-assembled monolayers as tunnel barriers, and we explore the extent to which organic molecules can be used as mechanically stable barriers. Mechanical stability, or at least a controlled degree of mechanical instability,⁵ will be essential in designing predictable and reliable molecular-scale devices. Achieving stability is a challenge because many molecules are intrinsically flexible, and the time-dependent forces associated with single charges moving through nanometer-scale devices can be large. We examine both single nanometer-scale tunnel junctions and also double-tunnel-junction devices incorporating a gold nanoparticle in a SAM barrier. The double-tunnel-junction samples are of particular interest because the barriers are sufficiently stable in some devices to allow detailed spectroscopic studies of electron tunneling through individual electron-in-a-box energy levels inside the gold nanoparticle at mK temperatures. This is the first time this has been achieved with a metal nanoparticle and SAM barriers. However, at larger source-drain voltages, we observe transport characteristics inconsistent with simple tunneling through fixed electronic states.

The samples are fabricated in a vertical geometry, through a bowl-shaped hole in a low-stress Si₃N₄ membrane.

The hole is formed using the process developed by Ralls *et al.*,⁶ which employs electron-beam lithography and reactive-ion etching with a CHF₃/O₂ plasma. The minimum diameter of the bowl-shaped hole is 3–10 nm.⁷ Metallization is done following a procedure similar to that of Zhou *et al.*⁴ To promote adhesion of the device to the Si₃N₄ membrane, ~10 Å of Cr or Ti is first evaporated on the bowl side of the sample (top of the sample in the inset of Fig. 1). Then a 2000 Å thick layer of Au is deposited to fill the bowl. After venting, the samples are placed in a 10 mM solution of SAMs (either 1,6-hexanedithiol, 1,8-octanedithiol, or 3-mercaptopropionic acid) in isopropanol, and are left to react for 24 h or more. After the formation of a monolayer, the samples are rinsed thoroughly with isopropanol and dried. To contact the top of the monolayer, ~20 Å of Au is evaporated at a rate of 1.7 Å/s, followed by 15 Å of Ti to promote adhesion. A 2000 Å thick layer of Au follows.

Simple tunnel junctions have been fabricated using 1,8-octanedithiol (21 devices) and 1,6-hexanedithiol (14 devices) as barriers. In both cases the current–voltage (*I*–*V*) curves measured up to 50 mV at 4.2 K are approximately linear, with *dI/dV* constant to within ~14%. Analysis of *I*–*V* characteristics measured up to 1 V gives a barrier height ranging from 4 to 5 eV (assuming that the barrier thickness is the

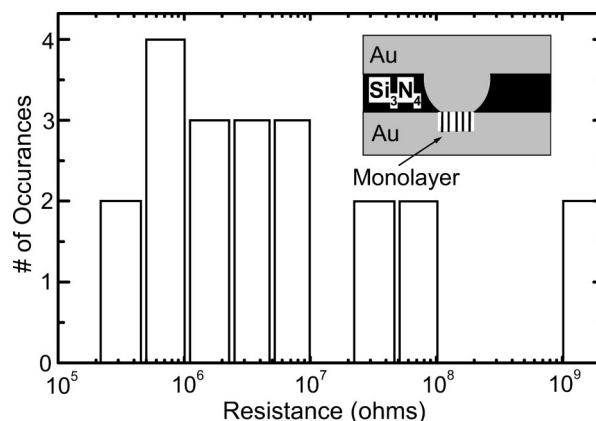


FIG. 1. Histogram of 1,8-octanedithiol tunnel junction resistances at 4.2 K. Inset: Device schematic.

^{a)}Electronic mail: jrp20@cornell.edu

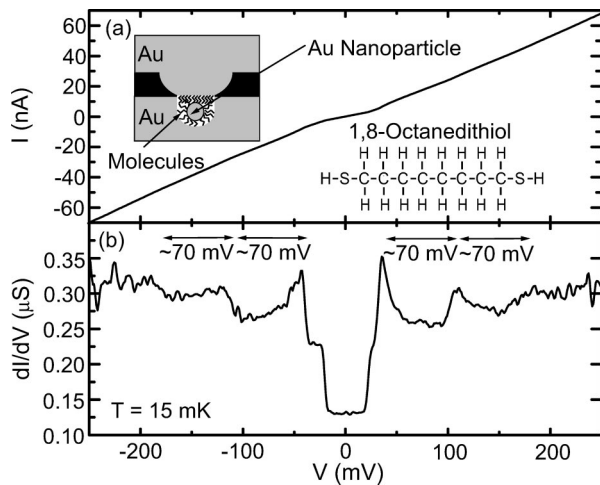


FIG. 2. (a) I - V curve for a device containing an Au nanoparticle with 1,8-octanedithiol barriers. (b) dI/dV - V determined by numerical differentiation. The regularly spaced peaks in dI/dV indicate tunneling through a single particle. Inset: Device schematic.

length of an octanedithiol molecule ~ 1.45 nm). A histogram of the resistances for the octanedithiol devices is shown in Fig. 1. Nineteen of the 21 devices have resistances between 300 k Ω and 60 M Ω . In the remaining two devices it is likely that a portion of the monolayer pulled away from the gold contact during cooldown, resulting in much higher resistances. The large resistances in all devices indicate that transport occurs via tunneling, since metallic pinholes would give resistances ≤ 13 k Ω . Based on the known packing density of thiol SAMs on gold surfaces ($\sim 5 \times 10^{14}$ molecules/cm 2)⁸ and the area of the junction region, we can estimate a resistance per molecule. The cross-sectional area for each batch of nanoholes was determined by evaporating copper on both sides of test samples (without a tunnel barrier) and converting the point-contact resistance to an area (A) using the Sharvin formula ($R = (h/e^2) 2\pi / (k_F^2 A)$).⁹ This estimate has been shown to be in good agreement with direct electron microscopy measurements.⁷ For the batch of samples in Fig. 1, we find a diameter of ~ 5 nm. Treating the molecules as parallel resistors we calculate an average resistance per molecule (for the nineteen lower resistance tunnel junctions) between 30 M Ω and 6 G Ω for the 1,8-octanedithiol devices. A similar analysis for the 1,6-hexanedithiol samples yields a resistance per molecule between 11 M Ω and 2 G Ω . T. Sato and Ahmed have calculated the resistance of a single molecule of 1,6-hexanedithiol to be ~ 30 G Ω .³ It is not surprising that the measured values are lower than theoretical predictions due to the possibility of imperfections in the SAM layer.

In a small percentage of samples ($\sim 2\%$) the results of the sample fabrication were not simple tunnel junctions with linear I - V curves, but rather I - V curves displaying evenly spaced Coulomb-blockade steps, characteristic of electron tunneling through a single metal nanoparticle (Fig. 2). In these samples it is likely that an Au particle nucleates on top of the self-assembled monolayer during the Au evaporation, and then nearby dithiols diffuse to cover the nanoparticle. The end result is a device with an Au nanoparticle connected to two macroscopic leads via organic linker molecules. The nonzero conductance in the blockade region in Fig. 2 is

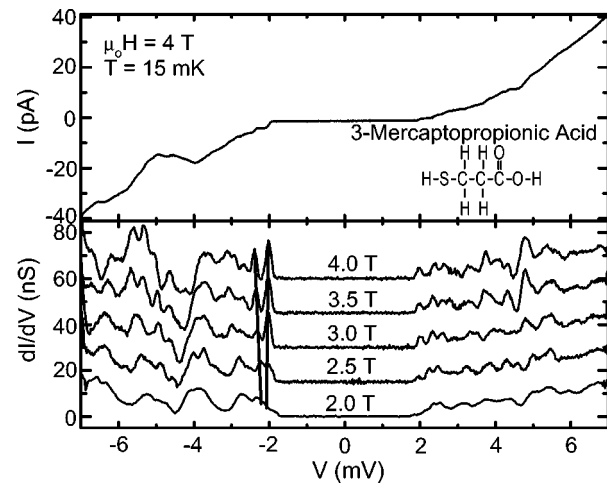


FIG. 3. Low-voltage transport characteristics for a Coulomb-blockade device with 3-mercaptopropionic-acid barriers. Well-resolved tunneling resonances are observed. The lines indicate a Zeeman doublet. The conductance curves are offset by 15 nS for clarity.

likely due to direct tunneling through the SAM barrier.

In nanoparticle tunnel junctions previously fabricated using aluminum oxide tunnel barriers, tunneling via individual electron-in-a-box energy levels within the nanoparticle produced a fine structure of discrete resonances in dI/dV at mK temperatures.^{10,11} In the SAM-barrier samples we also observe similar resonances. Figure 3 shows I - V and dI/dV - V curves at selected magnetic fields for a sample fabricated as described above with 3-mercaptopropionic acid forming the tunnel barriers. The first few resonances beyond the tunneling threshold for each sign of bias can be identified as tunneling through the same discrete states within the nanoparticle (in opposite directions), with the relative positions in voltage giving a capacitance ratio $C_1/C_2 = 1.02$. Another sign that the resonances are due to tunneling via discrete quantum states within the particle, rather than a more exotic cause, is the observation of Zeeman spin splitting as a function of applied magnetic field (well resolved for the first tunneling state above threshold). After accounting for the capacitive division of voltage across the tunnel junctions, we find an effective g -factor $g \sim 1.5 \pm 0.1$ for this Zeeman doublet. The ability to resolve narrow tunneling resonances and also the reproducibility of the spectra provide evidence that the nanoparticle is not undergoing large-scale motion in the course of these measurements, because such motion is known to shift the nanoparticle states¹² and would be expected to broaden any tunneling resonances.

This stability is not absolute, however. We occasionally observe large, sudden shifts in the threshold voltage required to overcome the Coulomb charging barrier. It is because of such shifts that the tunnel spectra in Fig. 3 are not displayed below 2 T or above 4 T. The negative differential conductance visible between -4 and -5 mV is also unusual compared to devices with Al $_2$ O $_3$ barriers, and is most easily explained as a voltage-dependent instability that shifts the Coulomb-staircase curve.

Figure 4 shows data from a Coulomb-blockade device fabricated with 1,8-octanedithiol. The capacitance ratio, $C_1/C_2 = 2.04$, for this sample is determined by measuring the peak widths as a function of temperature. From left to right,

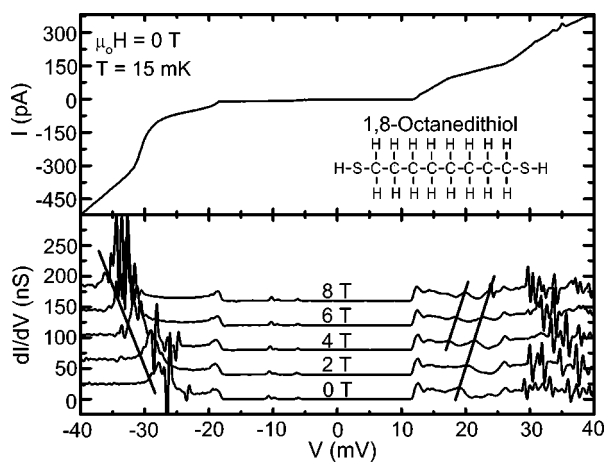


FIG. 4. Transport characteristics for a Coulomb-blockade device with 1,8-octanedithiol barriers. Three resonances, marked with lines, give anomalous g factors.

the three small conductance peaks near -9 mV give g factors of 1.4, 1.9, and 0.1. The g factors are accurate to within $\sim 10\%$, with most of the error due to the determination of the capacitance ratio. The variation in g factors can be explained as due to spin-orbit scattering.^{13,14} There are two surprising aspects of these data. One is the strong magnetic-field dependence of the three conductance peaks indicated with lines in Fig. 4. The large peak near -30 mV moves more than 7 mV over a field of 8 T; this gives (taking into account the capacitive voltage division) $g_{\text{eff}} \sim 20$. This is much too large to explain with any mechanism invoking simple tunneling through a fixed energy level on the nanoparticle, because spin-orbit scattering should always produce $g \leq 2$. The second surprising aspect, which appears to be associated with the onset of conduction at this anomalous peak, is a large increase in the conductance noise (not reproducible) with increasing source-drain bias. It is possible that transport in this regime is not due to simple tunneling, but may involve the motion of the Au grain, such as in the “shuttle mechanism” proposed by Gorelik *et al.*^{15,16} We can rule out effects of resonant tunneling through states in the barriers because we see no sign of this in the single-junction samples.

In conclusion, we have fabricated both single tunnel junctions and Coulomb-blockade devices using SAMs as the

tunnel barriers. The single-junction devices give resistances and barrier heights consistent with tunneling through a single layer of molecules. We have shown that it is possible to resolve well-defined electronic states in a metal nanoparticle using tunnel junctions formed from SAMs. With increasing source-drain voltages, the nanoparticle-tunneling devices exhibit anomalous behavior as a function of magnetic field and voltage. Further calculations are required to determine if this behavior is related to the “shuttle mechanism” proposed by Gorelik *et al.*¹⁵

The authors acknowledge helpful discussions with M. M. Deshmukh, S. Guéron, E. B. Myers, and A. Pasupathy. This work was supported by the Packard Foundation and the NSF (Grant No. DMR-9705059). One author (JRP) acknowledges the support of a NSF Graduate Research Fellowship. Sample fabrication was performed at the Cornell node of the National Nanofabrication Users Network, funded by the NSF.

- ¹D. L. Klein, R. Roth, A. K. L. Lim, A. P. Alivisatos, and P. L. McEuen, *Nature (London)* **389**, 699 (1997).
- ²L. G. M. Olofsson, S. H. M. Persson, A. Morpurgo, C. M. Marcus, D. Golubev, L. K. Gunnarsson, and Y. Yao, *J. Low Temp. Phys.* **118**, 343 (1999).
- ³T. Sato and H. Ahmed, *Appl. Phys. Lett.* **70**, 2759 (1997).
- ⁴C. Zhou, M. R. Desphande, M. A. Reed, L. Jones, and J. M. Tour, *Appl. Phys. Lett.* **71**, 611 (1997).
- ⁵C. P. Collier, E. W. Wong, M. Belohradsky, F. M. Raymo, J. F. Stoddart, P. J. Kuekes, R. S. Williams, and J. R. Heath, *Science* **285**, 391 (1999).
- ⁶K. S. Ralls, R. A. Buhrman, and R. C. Tiberio, *Appl. Phys. Lett.* **55**, 2459 (1989).
- ⁷M. M. Deshmukh, D. C. Ralph, M. Thomas, and J. Silcox, *Appl. Phys. Lett.* **75**, 1631 (1999).
- ⁸C. A. Widrig, C. A. Alves, and M. D. Porter, *J. Am. Chem. Soc.* **113**, 2805 (1991).
- ⁹A. G. M. Jansen, A. P. VanGelder, and P. Wyder, *J. Phys. C* **13**, 6073 (1980).
- ¹⁰D. C. Ralph, C. T. Black, and M. Tinkham, *Phys. Rev. Lett.* **74**, 3241 (1995).
- ¹¹D. Davidović and M. Tinkham, *Phys. Rev. Lett.* **83**, 1644 (1999).
- ¹²T. P. Bigioni, L. E. Harrell, W. G. Cullen, D. K. Guthrie, R. L. Whetten, and P. N. First, *Euro. Phys. J.* **6**, 355 (1999).
- ¹³D. G. Salinas, S. Guéron, D. C. Ralph, C. T. Black, and M. Tinkham, *Phys. Rev. B* **60**, 6137 (1999).
- ¹⁴P. W. Brouwer, X. Waintal, and B. I. Halperin, *Phys. Rev. Lett.* **85**, 369 (2000).
- ¹⁵L. Y. Gorelik, A. Isacsson, M. V. Voinova, B. Kasemo, R. I. Shekhter, and M. Jonson, *Phys. Rev. Lett.* **80**, 4526 (1998).
- ¹⁶M. T. Tuominen, R. V. Krotkov, and M. L. Breuer, *Phys. Rev. Lett.* **83**, 3025 (1999).